iScience

CellPress
OPEN ACCESS

Article

N6-methyladenosine modification of B7-H3 mRNA promotes the development and progression of colorectal cancer

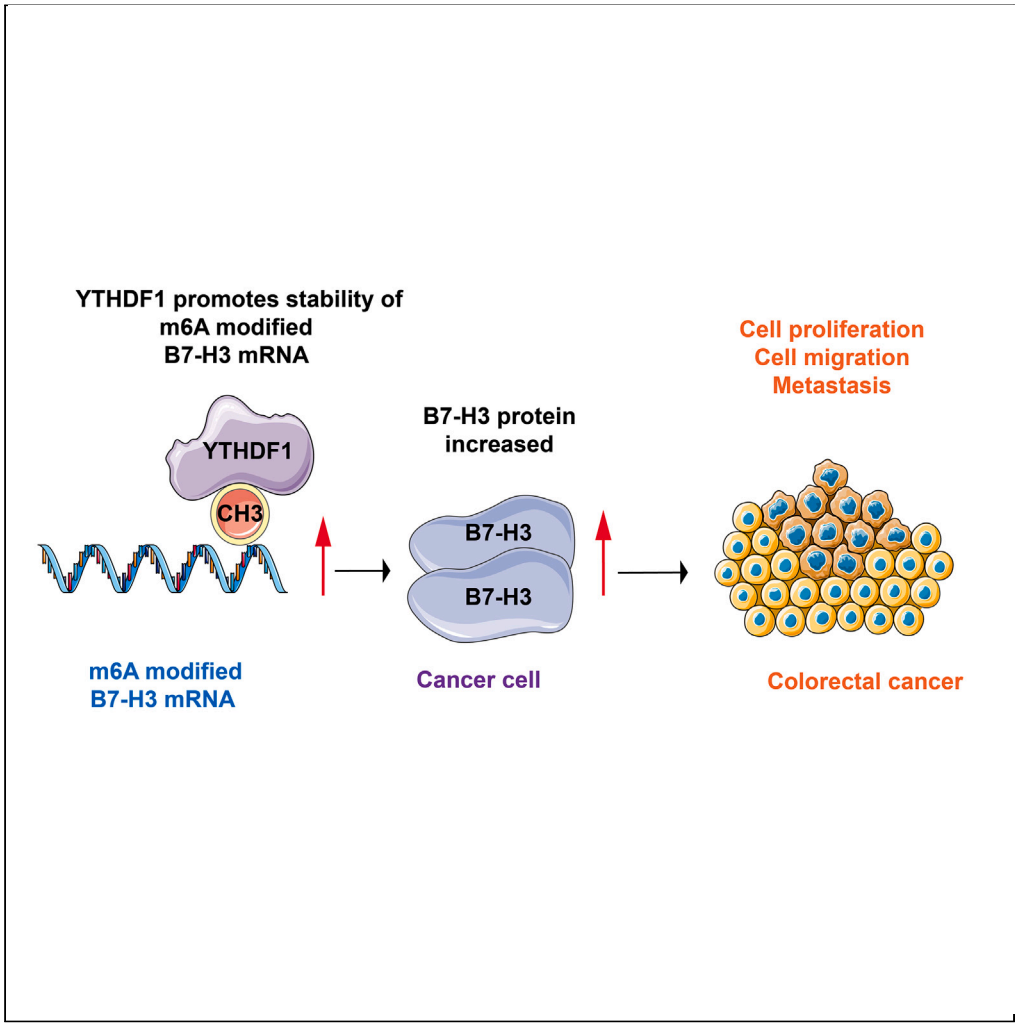

Rui Chen, Fei Su, Tao Zhang, Dongjin Wu, Jingru Yang, Quanlin Guan, Chen Chai

guanql@lzu.edu.cn (Q.G.)
chaich@lzu.edu.cn (C.C.)

Highlights

B7-H3 is overexpressed in CRC and is associated with a poor prognosis

B7-H3 promotes the malignant biological behaviors of CRC *in vivo* and *in vitro*

YTHDF1 protein binds to B7-H3 mRNA in an m6A-dependent manner

The YTHDF1-m6A-B7-H3 axis is crucial for CRC development and progression

Chen et al., iScience *27*, 108956
February 16, 2024
https://doi.org/10.1016/j.isci.2024.108956

iScience

CellPress
OPEN ACCESS

Article

N6-methyladenosine modification of B7-H3 mRNA promotes the development and progression of colorectal cancer

Rui Chen,[1,2,5] Fei Su,[1,2,5] Tao Zhang,[2,5] Dongjin Wu,[3,5] Jingru Yang,[1,2] Quanlin Guan,[1,4,6,*] and Chen Chai[3,*]

SUMMARY

B7-H3 is a common oncogene found in various cancer types. However, the molecular mechanisms underlying abnormal B7-H3 expression and colorectal cancer (CRC) progression need to be extensively explored. B7-H3 was upregulated in human CRC tissues and its abnormal expression was correlated with a poor prognosis in CRC patients. Notably, gain- and loss-of-function experiments revealed that B7-H3 knockdown substantially inhibited cell proliferation, migration, and invasion *in vitro*, whereas exogenous B7-H3 expression yielded contrasting results. In addition, silencing of B7-H3 inhibited tumor growth in a xenograft mouse model. Mechanistically, our study demonstrated that the N6-methyladenosine (m6A) binding protein YTHDF1 augmented B7-H3 expression in an m6A-dependent manner. Furthermore, rescue experiments demonstrated that reintroduction of B7-H3 considerably abolished the inhibitory effects on cell proliferation and invasion induced by silencing YTHDF1. Our results suggest that the YTHDF1-m6A-B7-H3 axis is crucial for CRC development and progression and may represent a potential therapeutic target for CRC treatment.

INTRODUCTION

Colorectal cancer (CRC) has the highest mortality rate among gastrointestinal malignancies and is the third most common cause of cancer-related death worldwide.[1] In China, patients with CRC are commonly diagnosed with advanced or metastatic disease, which results in poor prognosis and high relapse rates. Therefore, identifying specific biomarkers and therapeutic targets for CRC management requires immediate attention.

The seminal discovery of immune checkpoint molecules in the B7 family has revolutionized the clinical treatment of cancer. B7 homolog 3 (B7-H3 or CD276) has recently received widespread attention owing to its broad expression across multiple tumor types. Accumulating evidence indicates that B7-H3 is associated with embryonic and skeletal system maturation, angiogenesis, and control of tumor cell growth, migration, invasion, and cancer stemness.[2] B7-H3 is aberrantly expressed in various tumors, such as breast, lung, gastric, and brain cancers. B7-H3 primarily functions as a co-inhibitory molecule, accelerating tumor growth by preventing immune responses.[3] In addition, B7-H3 stimulates the invasion, metastasis, and resistance of tumor cells through non-immunological effects.[2,4] In CRC, patients with high B7-H3 expression exhibit a poorer prognosis and significant association with the progression and metastasis of CRC.[5–7] However, contradicting reports by Catalin M Lupu and colleagues suggest an antitumor role for B7-H3 in CRC. Therefore, further research is necessary to elucidate the precise role of B7-H3 in CRC.[8]

Adenosine methylation at the N6 position (m6A) is the most common mRNA modification in eukaryotic cells and regulates various RNA-related processes including transcription, maturation, translation, intracellular transport, degradation, and RNA stability.[9] Emerging evidence suggests that abnormal m6A modifications and related regulatory proteins play critical roles in cancer occurrence and development.[10] The fate of m6A-modified RNA is largely determined by the recognition of different m6A readers.[11] YTH N6-methyladenosine RNA-binding protein 1 (YTHDF1), one of the most abundant m6A readers, functionally binds to m6A-modified mRNA and accelerates target proteins translation.[12] Additionally, *in vitro* and *in vivo* experiments supported the role of YTHDF1 in promoting cancer initiation, progression, and metastasis.[13,14]

Although the relationship between m6A modification and colorectal tumorigenesis has been established in recent years, the precise molecular mechanisms of m6A-modified B7-H3 in CRC have not been sufficiently described. Based on previous studies, we explored the function

[1]The First Clinical Medical College of Lanzhou University, Lanzhou, Gansu 730000, P.R. China
[2]Department of Oncology, The First Hospital of Lanzhou University, Lanzhou, Gansu 730000, P.R. China
[3]People's Hospital of Suzhou New District, Suzhou, Jiangsu 215000, P.R. China
[4]Department of Oncology Surgery, The First Hospital of Lanzhou University, Lanzhou, Gansu 730000, P.R. China
[5]These authors contributed equally
[6]Lead contact
*Correspondence: guanql@lzu.edu.cn (Q.G.), chaich@lzu.edu.cn (C.C.)
https://doi.org/10.1016/j.isci.2024.108956

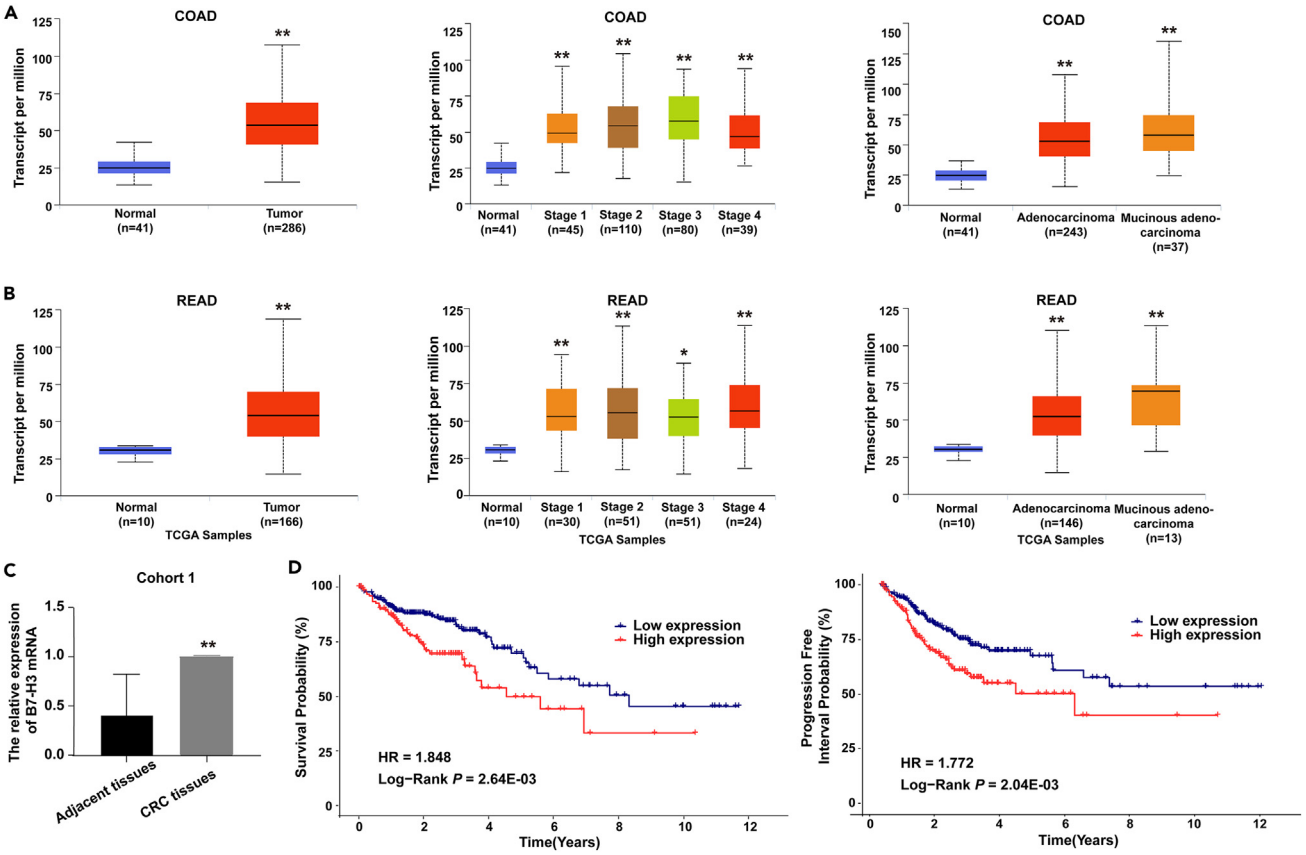

Figure 1. B7-H3 was highly expressed in COAD and READ

(A) Transcript levels of B7-H3 in primary COAD vs. healthy individuals, mRNA expression levels among stages, and mRNA levels in adenocarcinoma and mucinous adenocarcinoma of COAD from the TCGA database.

(B) Transcript levels of B7-H3 in primary READ vs. healthy individuals, mRNA expression levels among stages, and mRNA levels in adenocarcinoma and mucinous adenocarcinoma of READ from the TCGA database.

(C) Real-time PCR analysis of B7-H3 expression in 10 paired CRC tumor tissues and adjacent normal tissues.

(D) Kaplan-Meier analysis of OS time (left) and PFI time (right) based on B7-H3 expression. The values are significant at *p < 0.05, **p < 0.01 as indicated.

of B7-H3 in CRC tumorigenesis and progression and identified it as a downstream target of YTHDF1. Additionally, YTHDF1 maintains B7-H3 mRNA stability and inhibits mRNA decay. Overall, our results revealed the oncogenic role of m6A-modified B7-H3 and its regulatory mechanisms in CRC progression, suggesting that it is a potential therapeutic target for CRC.

RESULTS

B7-H3 was highly expressed in CRC

To investigate the B7-H3 expression in CRC, we analyzed the TCGA (The Cancer Genome Atlas) database. The results showed that B7-H3 mRNA levels were higher in primary tumors than in normal subjects (Figures 1A and 1B). Furthermore, at different tumor stages, the expression of B7-H3 mRNA differed and displayed an increasing tendency as disease malignancy increased (Figures 1A and 1B). Quantitative reverse transcription PCR (RT-qPCR) was conducted using fresh tissue samples from cohort 1 to detect B7-H3 mRNA levels. Similarly, B7-H3 mRNA expression was significantly upregulated in CRC tissues (Figure 1C). To explore the clinical implications of B7-H3 in CRC, we examined the correlation between B7-H3 and patient survival using the TCGA database. The results showed that patients with CRC with increased B7-H3 had worse overall survival (OS) and progression-free survival (Figure 1D). Collectively, the upregulated expression of B7-H3 leads to a worse prognosis in patients with CRC.

Next, we measured B7-H3 expression in CRC cell lines using RT-qPCR and western blotting. The findings indicated elevated B7-H3 mRNA expression levels in the CRC cell lines CACO2 and HCT116 compared to the normal mucosal FHC cells. However, no difference was observed in other CRC cell lines (Figure S1A). Interestingly, B7-H3 protein was expressed at a significantly higher level in CRC cell lines (CACO2, SW480, LOVO, SW620, HCT116, and DLD1) than in human colon epithelial FHC cells (Figure S1B). The outcomes of the western blotting analysis revealed that the B7-H3 protein exhibited its highest expression in the CACO2 and SW480 cell lines, while registering the lowest expression in the DLD1 cell line. Consequently, these three cell lines were chosen for subsequent experiments.

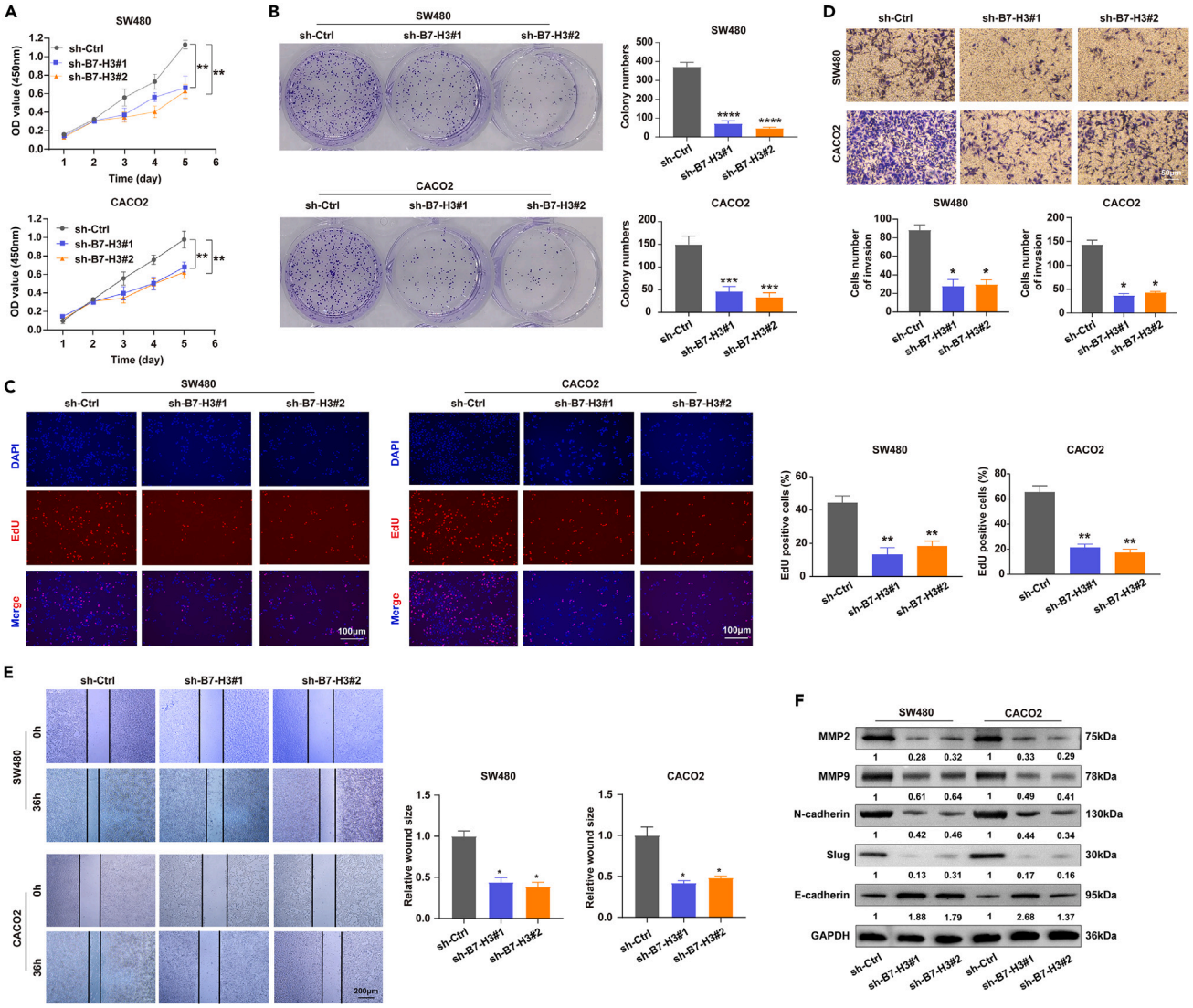

Figure 2. Knockdown of B7-H3 suppressed CRC cell proliferation, migration, and EMT

(A) Effects of B7-H3 knockdown on the proliferation of CRC cells, measured by CCK-8.

(B) Effects of B7-H3 knockdown on the colony formation of CRC cells, evaluated by colony formation assay.

(C) Effects of B7-H3 knockdown on the proliferation of CRC cells, measured by EdU assay.

(D) Effects of B7-H3 knockdown on the invasion of CRC cells, evaluated by transwell.

(E) Effects of B7-H3 knockdown on the migration of CRC cells, evaluated by wound healing assay.

(F) Effects of B7-H3 knockdown on the EMT-related proteins in CRC cells. Results are presented as means ± SD (n = 3 per group). GAPDH served as an internal control. The two-tailed Student's *t* test and one-way ANOVA were used for comparing two groups and more groups, respectively. *p < 0.05, **p < 0.01.

Knockdown of B7-H3 suppressed CRC cell proliferation, migration, and epithelial-mesenchymal transition

To explore the potential function of B7-H3 in CRC progression, we characterized the altered cellular phenotypes in CRC cells with B7-H3 knockdown. B7-H3 protein expression was highest in CACO2 cells and lowest in DLD1 cells (Figure S1B). To exclude off-target effects, we constructed stable B7-H3 knockdown models in CACO2 and SW480 cells using three distinct shRNA lentiviruses (sh-B7-H3#1, sh-B7-H3#2, and sh-B7-H3#3) and a control lentivirus (sh-Ctrl). Successful knockdown of B7-H3 was confirmed at both the mRNA and protein levels (Figures S1C and S1D). Knockdown of B7-H3 significantly reduced cell growth of CACO2 and SW480 cells, as determined by CCK-8 and EdU assays (Figures 2A and 2C). Similarly, B7-H3 silencing effectively suppressed the colony formation, invasion, and migration abilities of CRC cells (Figures 2B–2E) as indicated by colony formation, transwell, and wound healing assays. The epithelial-mesenchymal transition (EMT) pathway is closely associated with the progression and metastasis of CRC,[15] and B7-H3 has been reported to regulate EMT-related signaling pathways.[16] Therefore, we utilized western blotting to examine the regulatory effects of B7-H3 on key proteins within the EMT pathway in colorectal cancer. The results indicated that the downregulation of B7-H3 led to marked inhibition of the mesenchymal markers

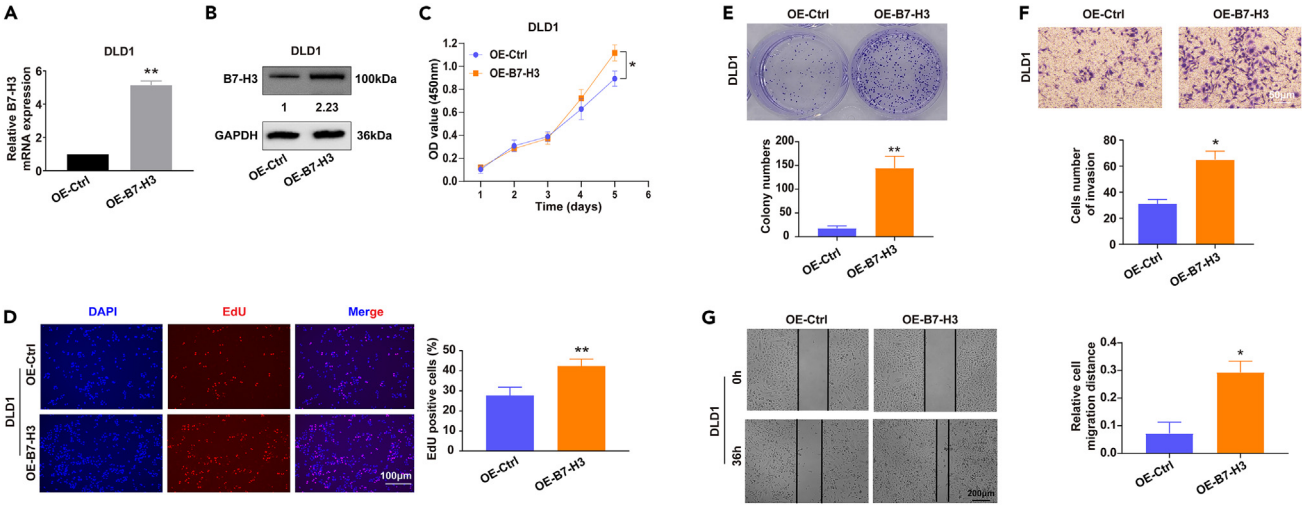

Figure 3. Overexpression of B7-H3 facilitated CRC cell proliferation, migration, and invasion

(A) The overexpression effect was verified at mRNA level using RT-qPCR.

(B) The overexpression effect was further verified at the protein level using western blotting assay.

(C) Effects of B7-H3 overexpression on the proliferation of CRC cells, measured by CCK-8 assay.

(D) Effects of B7-H3 overexpression on the proliferation of CRC cells, measured by EdU assay.

(E) Effects of B7-H3 overexpression on the colony formation of CRC cells, evaluated by colony formation assay.

(F) Effects of B7-H3 overexpression on the invasion of CRC cells, evaluated by Transwell.

(G) Effects of B7-H3 overexpression on the migration of CRC cells, evaluated by wound healing assay. Results were presented as means ± SD (n = 3 per group). GAPDH served as an internal control. The two-tailed Student's *t* test and one-way ANOVA were used for comparing two groups and more groups, respectively. *p < 0.05, **p < 0.01.

MMP-2, MMP-9, N-cadherin, and Slug. Conversely, the expression of the epithelial marker E-cadherin was upregulated by downregulation of B7-H3 (Figure 2F).

Overexpression of B7-H3 facilitated CRC cell proliferation and migration

Subsequently, we established stable B7-H3-overexpressing DLD1 cells. The overexpression of B7-H3 was validated by RT-qPCR and western blotting (Figures 3A and 3B). As predicted, upregulation of B7-H3 significantly promoted cell growth of DLD1 cells as indicated by CCK-8 and EdU assays (Figures 3C and 3D). Moreover, overexpression of B7-H3 markedly promoted CRC cell colony formation, invasion, and migration abilities (Figures 3E–3G) as evaluated by colony formation, transwell, and wound-healing assays. These findings indicated an oncogenic role of B7-H3 in CRC cell growth, migration, and metastasis.

Silencing B7-H3 repressed tumor growth *in vivo*

To further investigate the biological function of B7-H3 in CRC development *in vivo*, CACO2 cells stably infected with the lentivirus vector containing sh-Ctrl, sh-B7-H3#1, or sh-B7-H3#2 sequences were subcutaneously implanted into BALB/c nude mice. The tumor volumes in the sh-B7-H3 #1 and sh-B7-H3 #2 groups were significantly lower than those in the sh-control group from day 11 (Figures 4A and 4B). Mice in the sh-B7-H3#1 and sh-B7-H3#2 groups had remarkably lower tumor weights than those in the sh-Ctrl group (Figure 4C). Tumors were identified using H&E staining and immunohistochemistry (IHC) assays. IHC results indicated weaker Ki67 expression in tumor tissues in the sh-B7-H3 group than in the sh-Ctrl group (Figure 4D). These results revealed that B7-H3 is responsible for CRC tumor growth *in vivo*.

B7-H3 was a direct target of m6A reader YTHDF1

As previously described, upregulated B7-H3 in CRC promotes carcinogenesis and tumor progression. Therefore, we explored the mechanisms underlying the upregulation of B7-H3 in CRC. N6-methyladenosine (m6A) is a common post-transcriptional modification[9] ubiquitously occurring in most eukaryotic mRNA, tRNA, rRNA, and other non-coding RNAs. The functions of m6A modification include the regulation of gene expression, organism development, and cancer emergence.[17] To confirm whether abnormal modification of m6A regulates the expression of B7-H3, we first downloaded the m6A target gene sets from the M6A2Target database, and found that several B7-H3 m6A readers, including insulin-like growth factor-2 mRNA-binding protein family (IGF2BP1, IGF2BP2, and IGF2BP3), YTH domain-containing protein 1 (YTHDC1), and YTHDF1 (Table 1), may recognize m6A-modified B7-H3 and regulate its expression. Subsequently, we used the online predictive tool SRAMP (http://www.cuilab.cn/sramp) to identify several m6A modification sites in B7-H3 (Figure 5A). The transcript sequences of mature B7-H3 mRNA are listed in Table S1. Bioinformatics analysis demonstrated that YTHDF1 exhibited

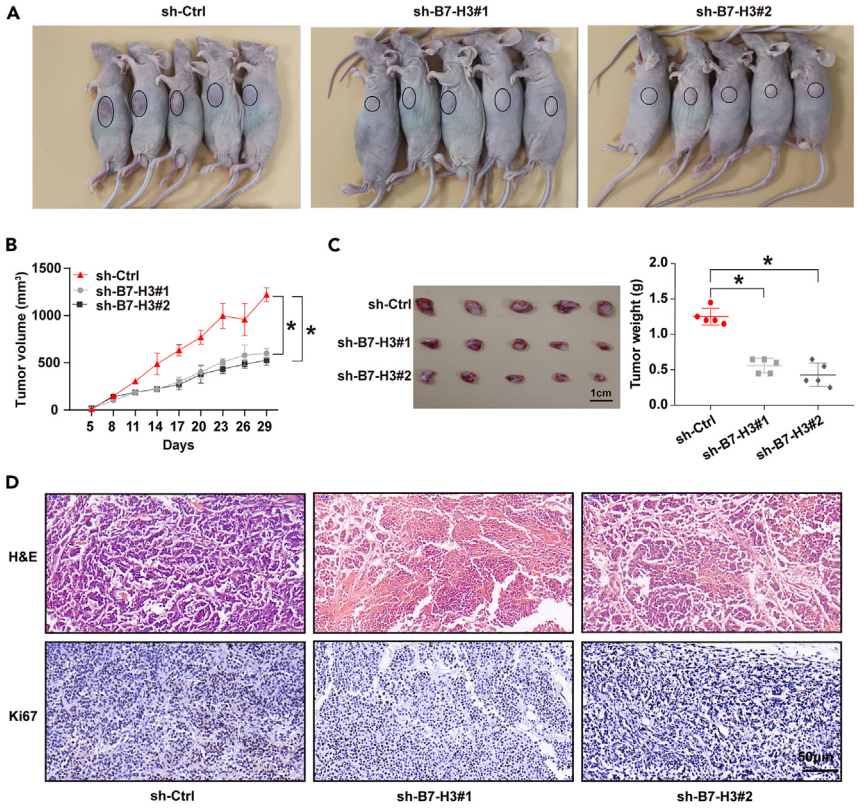

Figure 4. B7-H3 deficiency inhibited tumor growth *in vivo*

(A) Knockdown of B7-H3 effectively inhibited CRC subcutaneous tumor growth in nude mice (n = 5).

(B) The tumor volume was dramatically reduced on B7-H3 knockdown.

(C) Tumors dissected from the nude mice of each group were photographed at 29 days after transplantation (left) and the tumor weight was significantly decreased on B7-H3 knockdown (right).

(D) Representative histology images in mice subcutaneous tumor model (n = 5, 20×). Scale bar, 50 μm. Results are presented as means ± SD (n = 5 per group). The two-tailed Student's *t* test and one-way ANOVA were used for comparing two groups and more groups, respectively. *p < 0.05.

the highest correlation with B7-H3 in colon adenocarcinoma (r = 0.59, p < 0.0001) and rectal adenocarcinoma (r = 0.29, p = 0.004) (Figure 5B).

Because the RNA-binding protein YTHDF1 was identified as a "reader" in m6A RNA modification and played a specific role in controlling the fate of methylated mRNA,[14] we investigated whether RNA m6A modification affects the interaction between YTHDF1 and B7-H3. We validated the mRNA and protein levels of B7-H3 in YTHDF1-overexpressing (DLD1 and HCT116) and YTHDF1-knockdown CRC cell lines (CACO2 and SW480). As shown in Figures 5C and 5D, B7-H3 mRNA and protein levels were consistently regulated by YTHDF1 in the four CRC cell lines. Furthermore, we investigated whether m6A modification affects the stability of B7-H3 mRNA by

Table 1. The target genes that inferred from CLIP-seq, RIP-seq, CHIP-seq, or mass spectrometry

Binding

Species	Cell Line	Class	WER Name	Target Gene	Interaction	Method	Downstream Effect
Human	293T	Reader	IGF2BP1	B7-H3	Protein-RNA	CLIP-seq	No evidence
Human	293T	Reader	IGF2BP2	B7-H3	Protein-RNA	CLIP-seq	No evidence
Human	293T	Reader	IGF2BP3	B7-H3	Protein-RNA	CLIP-seq	No evidence
Human	293T	Reader	YTHDC1	B7-H3	Protein-RNA	CLIP-seq	No evidence
Human	A549	Reader	YTHDF1	B7-H3	Protein-RNA	RIP-seq	No evidence
Human	HeLa	Reader	YTHDF1	B7-H3	Protein-RNA	CLIP-seq	No evidence
Human	MDA-MB-231	Writer	METTL3	B7-H3	Protein-RNA	RIP-seq	No evidence

WERs: writers, erasers, and readers. "Protein-RNA" represents the genes inferred from various kinds of CLIP-seq or RIP-seq.

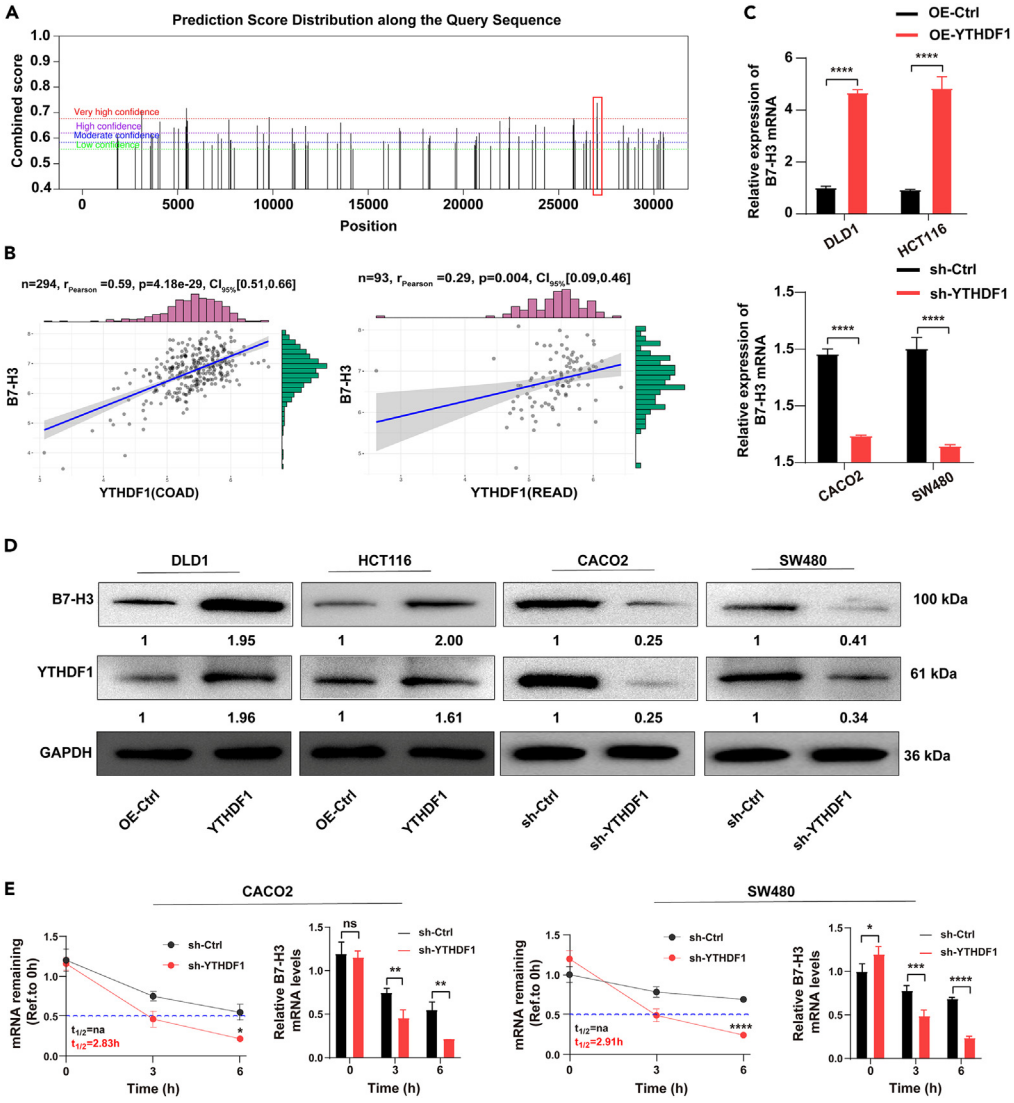

Figure 5. B7-H3 expression regulated by m6A methylation of RNA in CRC cells

(A) SRAMP analysis was used for prediction of the m6A methylation sites in B7-H3 mRNA.

(B) Correlation analysis between YTHDF1 expression and B7-H3 expression in COAD and READ datasets, respectively.

(C) The mRNA levels of B7-H3 in YTHDF1-overexpressing (upper) and YTHDF1 knockdown (lower) CRC cells were detected by RT-qPCR.

(D) The levels of the indicated proteins in YTHDF1-overexpressing and YTHDF1-knockdown CRC cells were detected by western blotting assay.

(E) After silencing YTHDF1 in CACO2 and SW480 cells, the mRNA half-lives and expression of B7-H3 were analyzed at the predetermined times following actinomycin D (5 μg/mL) treatment. GAPDH served as an internal control. Results are presented as means ± SD (n = 3 per group). The two-tailed Student's *t* test and one-way ANOVA were used for comparing two groups and more groups, respectively. *p < 0.05, **p < 0.01, ***p < 0.001, ****p < 0.0001.

treating CRC cells with actinomycin D, an inhibitor of transcription, for specific times. The results demonstrated that YTHDF1 silencing in CACO2 and SW480 cells decreased B7-H3 mRNA expression and continuously reduced its half-life (Figure 5E). Taken together, our data suggested that the methylated B7-H3 transcripts were directly recognized by the m6A "reader" YTHDF1, which maintained the stability of B7-H3 to prevent its degradation and naturally increase its expression via an m6A-YTHDF1-dependent mechanism.

Subsequently, we transfected sh-METTL3 into CACO2 and SW480 cells and measured B7-H3 protein expression in both cell lines. The results showed that protein levels of B7-H3 were significantly lower than those in the sh-Ctrl groups (Figure S2A). Furthermore, the methylated RNA immunoprecipitation-qPCR (MeRIP-qPCR) assay indicated that METTL3 knockdown decreased the enrichment of m6A-modified B7-H3 fragments in CACO2 and SW480 cells (Figure S2B). These results indicated that m6A methylation of RNA in CRC cells directly regulates B7-H3 expression.

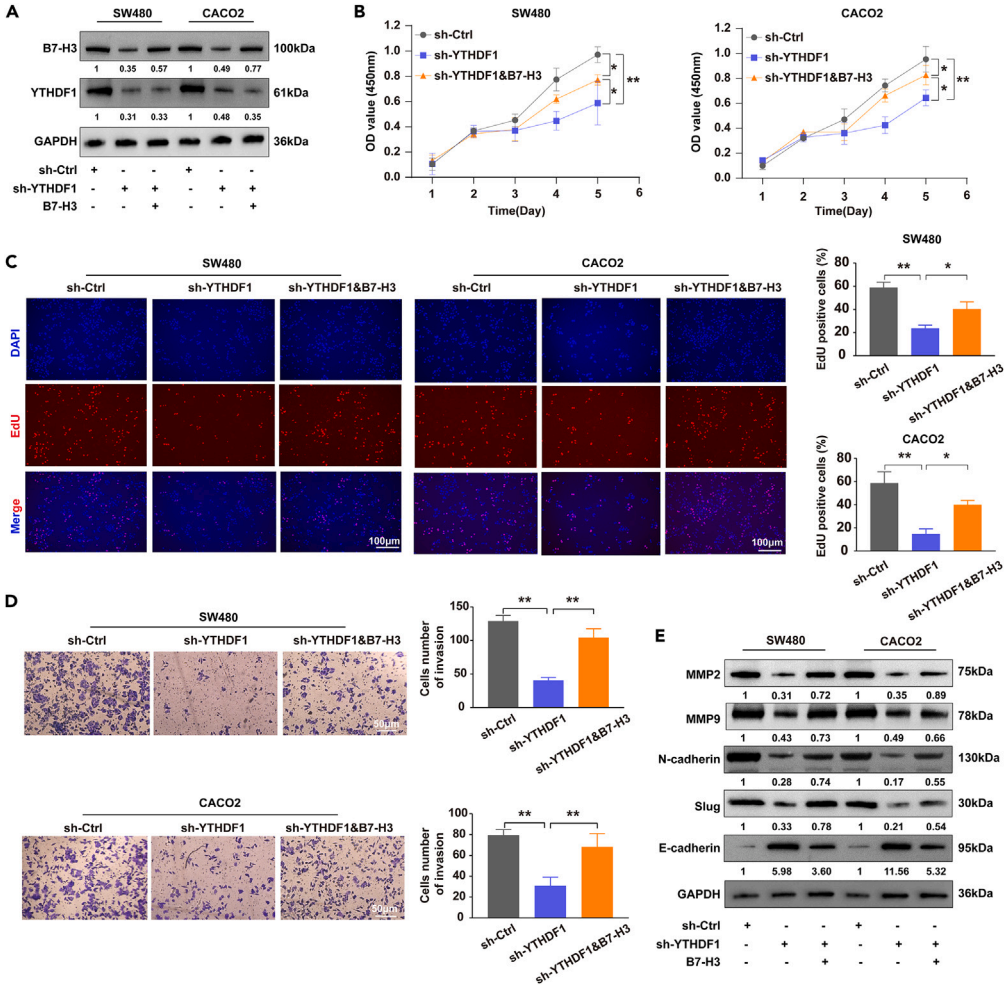

Figure 6. YTHDF1 promoted cell growth and migration of CRC cells dependent on B7-H3

(A) Western blotting detected the protein levels of YTHDF1 and B7-H3 in YTHDF1-knockdown or YTHDF1-knockdown with overexpression of B7-H3 CACO2 and SW480 cell lines.

(B) Cell growth was measured by CCK8 assay in CACO2 and SW480 cells described in (A).

(C) Cell growth was measured by EdU assay in CACO2 and SW480 cells described in (A). Scale bar, 100 μm.

(D) Transwell assays were used to measure abilities of migration of CRC cells described in (A). Scale bar, 50 μm.

(E) Western blotting assay for EMT-related proteins in CRC cells described in (A). GAPDH served as an internal control. All data are presented as the mean ± SD of at least three independent repetitions. The two-tailed Student's *t* test and one-way ANOVA were used for comparing between two groups and more groups, respectively. The values are significant at *p < 0.05, **p < 0.01.

B7-H3 overexpression blocked the cancer-suppressive effect of YTHDF1 silencing

We further verified the role of the YTHDF1/B7-H3 axis in CRC progression. We overexpressed B7-H3 in YTHDF1-knockdown CRC cells. The transfection efficiency was determined by western blotting (Figure 6A). Subsequently, CCK-8, EdU, transwell, and EMT assays were performed in sh-Ctrl, sh-YTHDF1 or sh-YTHDF1&B7-H3 CRC cells, respectively. These *in vitro* results demonstrated that YTHDF1 depletion inhibited the proliferation, migration, and EMT activities of CRC cells, which were at least partially abolished by overexpression of B7-H3 in these cells (Figures 6B–6E). We further investigated whether the YTHDF1/B7-H3 axis could affect the tumorigenesis and progression of colorectal cancer *in vivo*. We used a subcutaneous xenotransplantation model to evaluate the potential therapeutic effects of B7-H3 via intratumoral shRNA injection. The results showed that the tumor growth rate was slower, and the tumor volumes treated with B7-H3 shRNA were significantly lower than those of tumors in the control group (Figures S3A–S3C). Moreover, xenograft tumors were isolated and assessed by IHC staining, which showed reduced staining of mesenchymal phenotypic SNAIL and N-cadherin molecules and increased staining of epithelial phenotypic E-cadherin molecules in the B7-H3 shRNA-treated group (Figure S3D). Consistently, the downregulation of SNAIL and N-cadherin expression and the upregulation of E-cadherin expression suppressed by YTHDF1 deficiency were partially re-established after B7-H3 overexpression (Figure S3D). Collectively, these data indicate that B7-H3 as an oncogenic factor is a functionally critical downstream target of YTHDF1 that facilitates CRC tumorigenesis and progression.

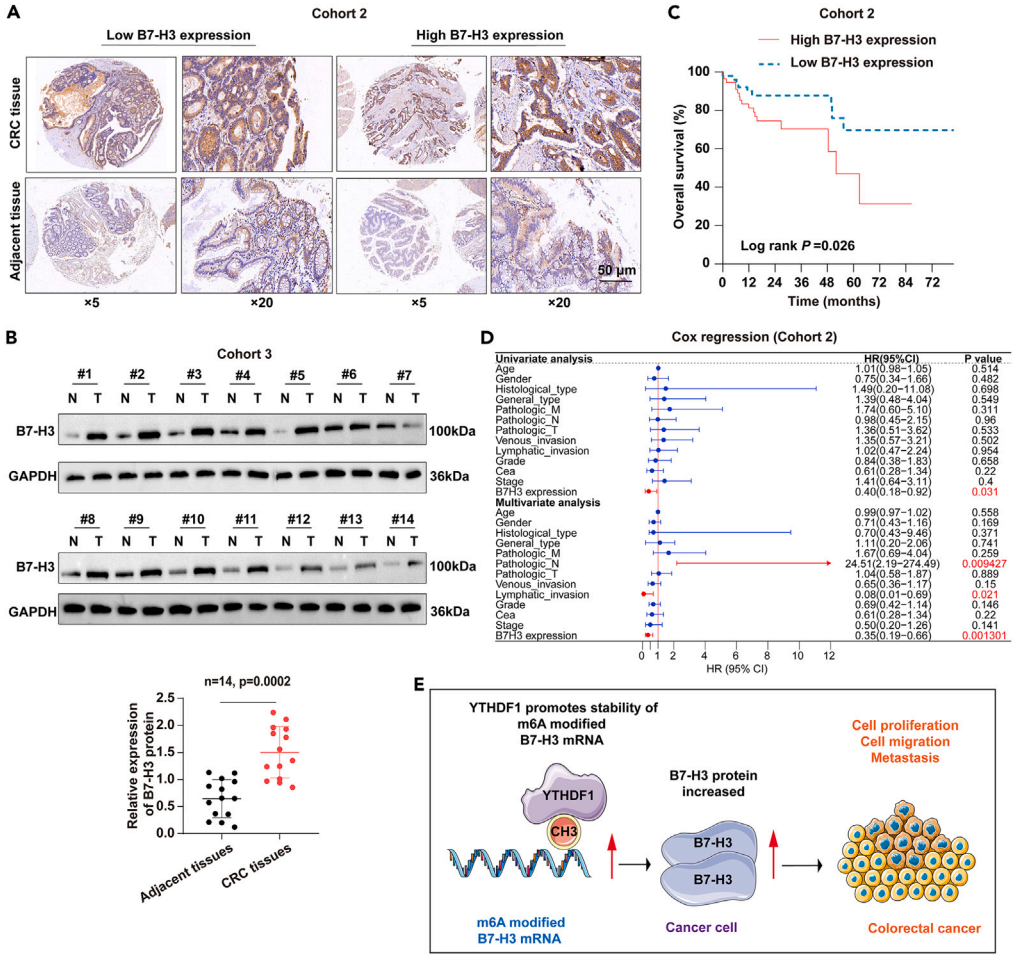

Figure 7. High B7-H3 expression predicted the poor prognosis of patients with CRC

(A) Typical images of B7-H3 protein in CRC and adjacent tissues stained by IHC. The B7-H3 protein was located in the cytoplasm of CRC and adjacent tissues.

(B) B7-H3 protein was quantitatively analyzed via western blotting assay in 14 pairs of fresh CRC and adjacent tissues (cohort 3).

(C) Kaplan-Meier analysis of overall survival (OS) for CRC patients (n = 109) based on the number of upregulated B7-H3 (Kaplan-Meier analysis with log rank test). B7-H3 expression was stratified by the individual medians from IHC analysis, and the patients were divided into two groups as indicated.

(D) Independent prognostic factor for overall survival of 109 patients with CRC, shown as a forest plot.

(E) Regulatory mechanism of the YTHDF1-m6A-B7-H3 axis in CRC. GAPDH served as an internal control. All data are presented as the mean ± SD of at least three independent repetitions. The two-tailed Student's *t* test was used for comparing between two groups.

YTHDF1-B7-H3 axis was associated with the stemness of CRC cells

To elucidate whether B7-H3 is associated with stem cell-like properties in CRC cells, we performed several experiments to test this cognition. The sphere formation assay revealed that YTHDF1 knockdown significantly inhibited the sphere-forming ability of CRC cells, which was restored by B7-H3 overexpression (Figure S4A). Further, western blotting revealed that B7-H3 overexpression in YTHDF1-knockdown CRC cells rescued the reduction in CSC surface stemness markers (such as ALDH, CD133, MYC, NANOG, and SOX2) (Figure S4B). Collectively, these results indicated the critical role of the YTHDF1/B7-H3 axis in promoting stemness in CRC.

B7-H3 was associated with a poor prognosis in patients with CRC

In addition to exploring the molecular carcinogenic molecular mechanism of B7-H3 in CRC, we assessed the influence of B7-H3 on the survival of patients with CRC. We collected 109 pairs of CRC tissues, including tumor and adjacent non-tumor tissue specimens (cohort 2), and examined B7-H3 expression by IHC. As shown in Figure 7A, the intensity of B7-H3 staining was strong in cancerous tissues, mainly localized in the cytoplasm, and was weak in the corresponding adjacent tissues. These findings corroborated that B7-H3 exerts a pro-tumorigenic role in the cytoplasm of CRC cells. However, high expression of B7-H3 was observed in 52.7% (58/109) of CRC tissues, whereas significant differences were observed in only 38.5% (42/109) of adjacent tissues ($\chi^2 = 4.729$, $p = 0.031$). We also explored B7-H3 protein levels in an independent cohort of 14 paired CRC tumors

and adjacent normal tissues (cohort 3). As shown in Figure 7B, the protein expression of B7-H3 in CRC tissues was significantly higher than that in adjacent tissues ($p < 0.001$).

To analyze the association between B7-H3 protein expression and clinicopathological features of patients with CRC, we divided the 109 patients into low and high B7-H3 expression groups based on the median expression of B7-H3 protein. Consistent with the aforementioned finding, we further found that B7-H3 expression was notably correlated with the prognosis of patients with CRC after grouping the CRC into B7-H3 "high expression" (n = 58) and "low expression" (n = 51) groups. We statistically analyzed the clinical and pathologic characteristics of the 109 CRC patients and found that high B7-H3 expression was strongly associated with abnormal carcinoembryonic antigen (CEA) levels, vascular invasion, and lymph node metastasis ($p < 0.05$); however, no significant correlation was observed between B7-H3 expression and other clinicopathological characteristics ($p > 0.05$) (Table 2). Follow-up analyses showed that patients with lower B7-H3 expression had a significantly longer overall survival period (Figure 7C). Finally, we constructed a Cox regression model using the CRC data to evaluate whether B7-H3 cells carried prognostically relevant information. Univariate and multivariate Cox regression analyses revealed that high B7-H3 expression was significantly correlated with poor prognosis for CRC patients and may serve as an independent prognostic factor for CRC ($p < 0.01$) (Figure 7D).

DISCUSSION

B7-H3, a member of the B7 family, also known as CD276, was initially identified as a costimulatory/coinhibitory immunoregulatory protein that plays a dual role in the immune system.[18] B7-H3 could promote the activation of T cells and the proliferation of IFN-γ.[19] Adenoviral B7-H3 therapy induced tumor-specific immune responses and reduced secondary metastasis in a murine model of colon cancer.[20] B7-H3 was considered a co-stimulatory molecule that is abundantly expressed in some solid cancers and is associated with improved treatment outcomes.[21] Compared to the co-stimulatory role of B7-H3, B7-H3 could inhibit the proliferation and activation of T cells and has a strong immunosuppressive effect.[22,23] Abnormal expression of B7-H3 enables cancer stem cells (CSCs) to escape immune surveillance, induce resistance of cancer cells to drugs, and promote EMT in malignant tumors.[24–26] B7-H3 remains an orphan ligand, although a potential receptor, TLT-2, has been detected in activated immune cells.[27] However, similar effects were not observed in another study involving human and murine B7-H3.[28] Therefore, considering that B7-H3 has many contradictory roles, identifying the specific receptors capable of binding B7-H3 is imperative. Herein, we explored the biological function of B7-H3 and aimed to identify its potential receptors in CRC. We found that B7-H3 expression was dramatically increased in all CRC samples and human CRC cell lines compared to their normal counterparts, and its high expression was significantly correlated with reduced OS, a high CEA level, and positive lymphatic metastasis. B7-H3 overexpression is an independent risk factor for poor outcomes in CRC patients. Importantly, our study revealed that the proliferation, migration, invasion, and EMT of CRC cells were effectively inhibited by shRNA-mediated B7-H3 knockdown but promoted by B7-H3 overexpression. Furthermore, our data indicated that B7-H3 is associated with subcutaneous tumorigenesis in nude mice. Therefore, B7-H3 may play essential roles in the proliferation, invasion, migration, and EMT of CRC cells.

Notably, the expression and activity of B7-H3 in tumors are regulated through various approaches. B7-H3 has been upregulated by ILT4,[29] TGF-β1,[30] PBK,[31] miR-124,[32] and PI3K/AKT/mTOR[29] signaling pathways, as well as epigenetic regulation.[33] All of these regulations promote cancer development in various solid tumors. The m6A-modified mRNA interacts with YTHDF1 by inserting its modified residues into the hydrophobic pocket of YTH domain Y.[34] YTHDF1 recognizes G (m6A) C and A (m6A) C RNA, thereby regulating the protein expression of m6A-modified target genes in both healthy and diseased conditions.[34,35] YTHDF1 modulates the translation efficiency of ARHGEF2 in human CRC cells,[36] thereby enhancing the carcinogenic and metastatic potential of CRC. In this study, we identified a unique epigenetic regulatory mechanism involving the YTHDF1-mediated m6A modification of B7-H3 during CRC progression. Using both cellular and animal models, we investigated the cellular and molecular mechanisms underlying B7-H3 mRNA m6A methylation in CRC cells. We found that B7-H3 is a critical downstream target of YTHDF1 and is regulated in an m6A-dependent manner. Moreover, METTL3 knockdown restricts B7-H3 m6A RNA methylation and ultimately suppresses B7-H3 protein expression. The positive correlation between B7-H3 and YTHDF1 indicates that the m6A reader YTHDF1 mediated the mRNA stability of B7-H3. Although YTHDF1 may play a carcinogenic role in CRC and regulate the expression and function of the downstream target B7-H3, overexpression of B7-H3 in YTHDF1-depleted cells can partially restore CRC proliferation, migration, and EMT phenotypes, which is consistent with the regulation of B7-H3 m6A in a previous study.[37] Therefore, we concluded that the YTHDF1-m6A-B7-H3 axis exists in the CRC.

A small group of cancer cells known as CSCs exhibit enhanced self-renewal capabilities and cause chemotherapy resistance, contributing to tumor recurrence and metastasis.[38,39] Tumor cell stemness can be regulated in multiple ways including classic pathways, epigenetic modification, and metabolic alterations. B7-H3, an immunoregulatory protein, regulates breast cancer stem cell enrichment and drug resistance through MVP-mediated MEK activation.[26] B7-H3 confers stemness to gastric cancer cells by promoting glutathione metabolism through the AKT/pAKT/Nrf2 pathway.[40] Colorectal cancer cells with higher B7-H3 levels express more cancer stem cell markers such as CD133, CD44, and Oct4.[41] In summary, B7-H3 induces cancer cells to express more stemness biomarkers, indicating that cancer cells exhibit greater self-renewal, distal metastatic capabilities, and drug resistance. CSCs possess self-renewal and multipotent differentiation characteristics, which may lead to tumorigenicity, progression, treatment resistance, recurrence, and metastasis. The acknowledged CSC markers ALDH, CD133, MYC, and SOX2 are highly expressed and involved in maintaining the properties of tumor-initiating cells and promoting the proliferation and metastasis of CRC.[42] However, the effect of the YTHDF1-m6A-B7-H3 axis on CRC stemness remains unclear. In our study, we showed that YTHDF1 silencing prevents CSC sphere formation and reduces the expression of these surface antigens. Nonetheless, B7-H3 overexpression in YTHDF1-knockdown CRC cells led to increased sphere formation and partial restoration of stemness markers. Therefore, the aforementioned

Table 2. Clinicopathological characteristics of CRC patients with differential B7-H3 expression

	B7-H3 Expression		
Characteristic	High (N = 58)	Low (N = 51)	p-value
Age (year)			
<65	28 (48.3)	22 (43.1)	0.73
≧ 65	30 (51.7)	29 (56.9)	
Gender			
Male	32 (55.2)	33 (64.7)	0.414
Female	26 (44.8)	18 (35.3)	
Histological_type			
Adenocarcinoma	57 (98.3)	49 (96.1)	0.91
Mucinous adenocarcinoma	1 (1.7)	2 (3.9)	
General_type			
Protrude	18 (31.0)	5 (9.8)	**0.013**
Ulcerative	40 (69.0)	46 (90.2)	
T stage			
T1-T2	14 (24.1)	13 (25.5)	0.82
T3-T4	44 (75.9)	37 (72.5)	
N stage			
N0	31 (53.4)	14 (27.5)	**0.008**
N1-N2	27 (46.6)	36 (70.6)	
M stage			
M0	50 (86.2)	40 (78.4)	0.908
M1	7 (12.1)	6 (11.8)	
CEA level			
Abnormal	35 (60.3)	17 (33.3)	**0.009**
Normal	23 (39.7)	34 (66.7)	
Vasucular invasion			
YES	18 (31.0)	6 (11.8)	**0.028**
NO	40 (69.0)	45 (88.2)	
Lymph_node invasion			
YES	27 (46.6)	35 (68.6)	**0.033**
NO	31 (53.4)	16 (31.4)	
Grade			
Moderate	23 (39.7)	21 (41.2)	0.794
Poor	34 (58.6)	28 (54.9)	
TNM stage			
I-II	29 (50.0)	20 (39.2)	0.349
III-IV	29 (50.0)	31 (60.8)	

results indicate that B7-H3 might be a potential CSC marker because of its functions in maintaining CSC stemness and that the YTHDF1-m6A-B7-H3 axis may have therapeutic potential for treating CRC.

In summary, our study identified an oncogenic role for the immune checkpoint B7-H3 in the progression of CRC. The combined network of "writer" METTL3, "reader" YTHDF1, and "target" B7-H3 highlighted an innovative m6A-dependent regulatory mechanism in CRC progression (Figure 7E). Considering the widespread B7-H3 upregulation in CRC and its pro-oncogenic role in CRC progression, targeting the YTHDF1-m6A-B7-H3 axis might be a promising therapeutic strategy for CRC.

Limitation of the study

Our study demonstrates that YTHDF1-mediated methylation of B7-H3 mRNA promotes tumor growth and metastasis in CRC, which provides an innovative m6A-dependent regulatory mechanism in the progression of CRC. However, the role of m6A in the regulation of antitumor immune responses remains unclear. Moreover, the role of YTHDF1 in regulating other genes in the immune pathway needs to be explored. In addition, the roles of other m6A-related genes in immune processes, including the regulatory effects of B7-H3, remain unclear. Our study relied only on *in vitro* experiments and animal models without further validation of clinical patient data and future studies are needed to achieve early clinical translation.

STAR★METHODS

Detailed methods are provided in the online version of this paper and include the following:

- KEY RESOURCES TABLE
- RESOURCE AVAILABILITY
  - Lead contact
  - Materials availability
  - Data and code availability
- EXPERIMENTAL MODEL AND STUDY PARTICIPANT DETAILS
  - Clinical samples
  - Animals
- METHOD DETAILS
  - Cell culture
  - RT-qPCR
  - Western blotting
  - Lentiviruses and cell transfection
  - Cell growth and proliferation assays
  - Transwell assay
  - Wound healing assay
  - Methylated RNA immunoprecipitation-qPCR (MeRIP-qPCR)
  - Animal experiments
  - The mRNA stability assay
  - Tumor sphere formation assay
  - H&E and IHC staining
  - Bioinformatics analyses
- QUANTIFICATION AND STATISTICAL ANALYSIS

SUPPLEMENTAL INFORMATION

Supplemental information can be found online at https://doi.org/10.1016/j.isci.2024.108956.

ACKNOWLEDGMENTS

The authors would like to thank acknowledge m6A2Target, TCGA, SRAMP, and NCBI database for providing their platforms and contributors for uploading their meaningful datasets. This work reported in this publication was supported by (1) Science Innovation Fund of People's Hospital of Suzhou New District (SGY2020C03), (2) Natural Science Foundation of Gansu Province (22JR5RA909, 21JR11RA077, and 21JR7RA386), (3) Gansu Province Higher Education Innovation Ability Improvement Project (2020B-009; 2021B-001), (4) Clinical Medical Science and Technology Development Foundation of Jiangsu University (JLY2021118) and (5) Science and Technology Project of Suzhou city (SKJY2021039).

AUTHOR CONTRIBUTIONS

R.C.: conceived and supervised the project, writing – original draft, writing – review & editing, and visualization. F.S.: data analysis, writing – original draft, and writing – review & editing. T.Z.: methodology, validation, formal analysis, and writing – review & editing. C.C.: investigation and writing – review & editing. D.W.: conceptualization, formal analysis, and data curation. J.Y.: software. Q.G.: conceptualization, formal analysis, data curation, writing – original draft, writing – review & editing, visualization, supervision, and project administration. All authors read and approved the final paper.

DECLARATION OF INTERESTS

The authors declare that they have no known competing financial interests or personal relationships that could have appeared to influence the work reported in this paper.

Received: July 26, 2023
Revised: December 29, 2023
Accepted: January 15, 2024
Published: January 18, 2024

REFERENCES

1. Deo, S.V.S., Sharma, J., and Kumar, S. (2022). GLOBOCAN 2020 Report on Global Cancer Burden: Challenges and Opportunities for Surgical Oncologists. Ann. Surg Oncol. *29*, 6497–6500.
2. Feng, R., Chen, Y., Liu, Y., Zhou, Q., and Zhang, W. (2021). The role of B7-H3 in tumors and its potential in clinical application. Int. Immunopharm. *101*, 108153.
3. Kontos, F., Michelakos, T., Kurokawa, T., Sadagopan, A., Schwab, J.H., Ferrone, C.R., and Ferrone, S. (2021). B7-H3: An Attractive Target for Antibody-based Immunotherapy. Clin. Cancer Res. *27*, 1227–1235.
4. Ma, Y., Wang, R., Lu, H., Li, X., Zhang, G., Fu, F., Cao, L., Zhan, S., Wang, Z., Deng, Z., et al. (2020). B7-H3 promotes the cell cycle-mediated chemoresistance of colorectal cancer cells by regulating CDC25A. J. Cancer *11*, 2158–2170.
5. Wang, J., Chen, X., Xie, C., Sun, M., Hu, C., Zhang, Z., Luan, L., Zhou, J., Zhou, J., Zhu, X., et al. (2021). MicroRNA miR-29a Inhibits Colon Cancer Progression by Downregulating B7-H3 Expression: Potential Molecular Targets for Colon Cancer Therapy. Mol. Biotechnol. *63*, 849–861.
6. Lu, H., Shi, T., Wang, M., Li, X., Gu, Y., Zhang, X., Zhang, G., and Chen, W. (2020). B7-H3 inhibits the IFN-gamma-dependent cytotoxicity of Vgamma9Vdelta2 T cells against colon cancer cells. OncoImmunology *9*, 1748991.
7. Bin, Z., Guangbo, Z., Yan, G., Huan, Z., Desheng, L., and Xueguang, Z. (2014). Overexpression of B7-H3 in CD133+ colorectal cancer cells is associated with cancer progression and survival in human patients. J. Surg. Res. *188*, 396–403.
8. Lupu, C.M., Eisenbach, C., Kuefner, M.A., Schmidt, J., Lupu, A.D., Stremmel, W., and Encke, J. (2006). An orthotopic colon cancer model for studying the B7-H3 antitumor effect in vivo. J. Gastrointest. Surg. *10*, 635–645.
9. An, Y., and Duan, H. (2022). The role of m6A RNA methylation in cancer metabolism. Mol. Cancer *21*, 14.
10. Zhang, X., Su, H., Chen, H., Li, Q., Liu, X., Zhang, L., Wu, W.K.K., Chan, M.T.V., and Chen, H. (2022). RNA Modifications in Gastrointestinal Cancer: Current Status and Future Perspectives. Biomedicines *10*, 1918.
11. Patil, D.P., Pickering, B.F., and Jaffrey, S.R. (2018). Reading m(6)A in the Transcriptome: m(6)A-Binding Proteins. Trends Cell Biol. *28*, 113–127.
12. Pi, J., Wang, W., Ji, M., Wang, X., Wei, X., Jin, J., Liu, T., Qiang, J., Qi, Z., Li, F., et al. (2021). YTHDF1 Promotes Gastric Carcinogenesis by Controlling Translation of FZD7. Cancer Res. *81*, 2651–2665.
13. Ji, H., Zhang, J.A., Liu, H., Li, K., Wang, Z.W., and Zhu, X. (2022). Comprehensive characterization of tumor microenvironment and m6A RNA methylation regulators and its effects on PD-L1 and immune infiltrates in cervical cancer. Front. Immunol. *13*, 976107.
14. Chen, D., Cheung, H., Lau, H.C.H., Yu, J., and Wong, C.C. (2022). N(6)-Methyladenosine RNA-Binding Protein YTHDF1 in Gastrointestinal Cancers: Function, Molecular Mechanism and Clinical Implication. Cancers *14*, 3489.
15. Tian, X., Wang, J., Jiang, L., Jiang, Y., Xu, J., and Feng, X. (2022). Chemokine/GPCR Signaling-Mediated EMT in Cancer Metastasis. JAMA Oncol. *2022*, 2208176.
16. Yu, T.T., Zhang, T., Lu, X., and Wang, R.Z. (2018). B7-H3 promotes metastasis, proliferation, and epithelial-mesenchymal transition in lung adenocarcinoma. OncoTargets Ther. *11*, 4693–4700.
17. Ru, W., Zhang, X., Yue, B., Qi, A., Shen, X., Huang, Y., Lan, X., Lei, C., and Chen, H. (2020). Insight into m(6)A methylation from occurrence to functions. Open Biol. *10*, 200091.
18. Ding, J., Sun, Y., Sulaiman, Z., Li, C., Cheng, Z., and Liu, S. (2023). Comprehensive Analysis Reveals Distinct Immunological and Prognostic Characteristics of CD276/B7-H3 in Pan-Cancer. Int. J. Gen. Med. *16*, 367–391.
19. Chapoval, A.I., Ni, J., Lau, J.S., Wilcox, R.A., Flies, D.B., Liu, D., Dong, H., Sica, G.L., Zhu, G., Tamada, K., and Chen, L. (2001). B7-H3: a costimulatory molecule for T cell activation and IFN-gamma production. Nat. Immunol. *2*, 269–274.
20. Lupu, C.M., Eisenbach, C., Lupu, A.D., Kuefner, M.A., Hoyler, B., Stremmel, W., and Encke, J. (2007). Adenoviral B7-H3 therapy induces tumor specific immune responses and reduces secondary metastasis in a murine model of colon cancer. Oncol. Rep. *18*, 745–748.
21. Liang, J., Liu, Z., Pei, T., Xiao, Y., Zhou, L., Tang, Y., Zhou, C., Wu, K., Zhang, F., Zhang, F., et al. (2020). Clinicopathological and Prognostic Characteristics of CD276 (B7-H3) Expression in Adrenocortical Carcinoma. Dis. Markers *2020*, 5354825.
22. Ma, J., Ma, P., Zhao, C., Xue, X., Han, H., Liu, C., Tao, H., Xiu, W., Cai, J., and Zhang, M. (2016). B7-H3 as a promising target for cytotoxicity T cell in human cancer therapy. Oncotarget *7*, 29480–29491.
23. Loos, M., Hedderich, D.M., Friess, H., and Kleeff, J. (2010). B7-h3 and its role in antitumor immunity. Clin. Dev. Immunol. *2010*, 683875.
24. Chen, H., Duan, X., Deng, X., Huang, Y., Zhou, X., Zhang, S., Zhang, X., Liu, P., Yang, C., Liu, G., et al. (2023). EBV-upregulated B7-H3 inhibits NK cell-mediated antitumor function and contributes to nasopharyngeal carcinoma progression. Cancer Immunol. Res. *11*, 830–846.
25. Liao, H., Ding, M., Zhou, N., Yang, Y., and Chen, L. (2022). B7-H3 promotes the epithelial-mesenchymal transition of NSCLC by targeting SIRT1 through the PI3K/AKT pathway. Mol. Med. Rep. *25*, 79.
26. Liu, Z., Zhang, W., Phillips, J.B., Arora, R., McClellan, S., Li, J., Kim, J.H., Sobol, R.W., and Tan, M. (2019). Immunoregulatory protein B7-H3 regulates cancer stem cell enrichment and drug resistance through MVP-mediated MEK activation. Oncogene *38*, 88–102.
27. Zhang, G., Wang, J., Kelly, J., Gu, G., Hou, J., Zhou, Y., Redmond, H.P., Wang, J.H., and Zhang, X. (2010). B7-H3 augments the inflammatory response and is associated with human sepsis. J. Immunol. *185*, 3677–3684.
28. Leitner, J., Klauser, C., Pickl, W.F., Stöckl, J., Majdic, O., Bardet, A.F., Kreil, D.P., Dong, C., Yamazaki, T., Zlabinger, G., et al. (2009). B7-H3 is a potent inhibitor of human T-cell activation: No evidence for B7-H3 and TREML2 interaction. Eur. J. Immunol. *39*, 1754–1764.
29. Zhang, P., Yu, S., Li, H., Liu, C., Li, J., Lin, W., Gao, A., Wang, L., Gao, W., and Sun, Y. (2015). ILT4 drives B7-H3 expression via PI3K/AKT/mTOR signalling and ILT4/B7-H3 co-expression correlates with poor prognosis in non-small cell lung cancer. FEBS Lett. *589*, 2248–2256.
30. Zhou, X., Mao, Y., Zhu, J., Meng, F., Chen, Q., Tao, L., Li, R., Fu, F., Liu, C., Hu, Y., et al. (2016). TGF-β1 promotes colorectal cancer immune escape by elevating B7-H3 and B7-H4 via the miR-155/miR-143 axis. Oncotarget *7*, 67196–67211.
31. Wang, M.Y., Qi, B., Wang, F., Lin, Z.R., Li, M.Y., Yin, W.J., Zhu, Y.Y., He, L., Yu, Y., Yang, F., et al. (2021). PBK phosphorylates MSL1 to elicit epigenetic modulation of CD276 in nasopharyngeal carcinoma. Oncogenesis *10*, 9.
32. Wang, L., Kang, F.B., Sun, N., Wang, J., Chen, W., Li, D., and Shan, B.E. (2016). The tumor suppressor miR-124 inhibits cell proliferation and invasion by targeting B7-H3 in osteosarcoma. Tumour Biol. *37*, 14939–14947.
33. Wang, Z., Wang, Z., Zhang, C., Liu, X., Li, G., Liu, S., Sun, L., Liang, J., Hu, H., Liu, Y., et al. (2018). Genetic and clinical characterization of B7-H3 (CD276) expression and epigenetic regulation in diffuse brain glioma. Cancer Sci. *109*, 2697–2705.
34. Chen, Z., Zhong, X., Xia, M., and Zhong, J. (2021). The roles and mechanisms of the m6A reader protein YTHDF1 in tumor biology and human diseases. Mol. Ther. Nucleic Acids *26*, 1270–1279.
35. Xu, C., Liu, K., Ahmed, H., Loppnau, P., Schapira, M., and Min, J. (2015). Structural Basis for the Discriminative Recognition of N6-Methyladenosine RNA by the Human YT521-B Homology Domain Family of Proteins. J. Biol. Chem. *290*, 24902–24913.
36. Wang, S., Gao, S., Zeng, Y., Zhu, L., Mo, Y., Wong, C.C., Bao, Y., Su, P., Zhai, J., Wang, L., et al. (2022). N6-Methyladenosine Reader YTHDF1 Promotes ARHGEF2 Translation and RhoA Signaling in Colorectal Cancer. Gastroenterology *162*, 1183–1196.
37. Zhou, Y., Zhou, H., Shi, J., Guan, A., Zhu, Y., Hou, Z., and Li, R. (2021). Decreased m6A Modification of CD34/CD276(B7-H3) Leads to Immune Escape in Colon Cancer. Front. Cell Dev. Biol. *9*, 715674.

38. Humphries, A., and Wright, N.A. (2008). Colonic crypt organization and tumorigenesis. Nat. Rev. Cancer *8*, 415–424.
39. Ricci-Vitiani, L., Fabrizi, E., Palio, E., and De Maria, R. (2009). Colon cancer stem cells. J. Mol. Med. *87*, 1097–1104.
40. Xia, L., Chen, Y., Li, J., Wang, J., Shen, K., Zhao, A., Jin, H., Zhang, G., Xi, Q., Xia, S., et al. (2023). B7-H3 confers stemness characteristics to gastric cancer cells by promoting glutathione metabolism through AKT/pAKT/Nrf2 pathway. Chin. Med. J. *136*, 1977–1989.
41. Jiang, B., Zhang, T., Liu, F., Sun, Z., Shi, H., Hua, D., and Yang, C. (2016). The co-stimulatory molecule B7-H3 promotes the epithelial-mesenchymal transition in colorectal cancer. Oncotarget *7*, 31755–31771.
42. Walcher, L., Kistenmacher, A.K., Suo, H., Kitte, R., Dluczek, S., Strauß, A., Blaudszun, A.R., Yevsa, T., Fricke, S., and Kossatz-Boehlert, U. (2020). Cancer Stem Cells-Origins and Biomarkers: Perspectives for Targeted Personalized Therapies. Front. Immunol. *11*, 1280.
43. Livak, K.J., and Schmittgen, T.D. (2001). Analysis of relative gene expression data using real-time quantitative PCR and the 2(-Delta Delta C(T)) Method. Methods *25*, 402–408.
44. Liu, J., Eckert, M.A., Harada, B.T., Liu, S.M., Lu, Z., Yu, K., Tienda, S.M., Chryplewicz, A., Zhu, A.C., Yang, Y., et al. (2018). m(6)A mRNA methylation regulates AKT activity to promote the proliferation and tumorigenicity of endometrial cancer. Nat. Cell Biol. *20*, 1074–1083.
45. Lama, G., Upadhyaya, P., Karki, S., and Pradhan, A. (2021). Deeper Sections: Its Frequency and Diagnostic Utility in Histopathology of Noncutaneous Small Biopsy Specimen in a Tertiary Hospital in Nepal. Adv. Met. Med. *2021*, 5926047.
46. Schricker, S., Oberacker, T., Fritz, P., Ketteler, M., Alscher, M.D., and Schanz, M. (2022). Peritoneal Expression of SGLT-2, GLUT1, and GLUT3 in Peritoneal Dialysis Patients. Kidney Blood Press. Res. *47*, 125–134.
47. Kusuhara, S., Igawa, S., Ichinoe, M., Nagashio, R., Kuchitsu, Y., Hiyoshi, Y., Shiomi, K., Murakumo, Y., Saegusa, M., Satoh, Y., et al. (2021). Prognostic significance of galectin-3 expression in patients with resected NSCLC treated with platinum-based adjuvant chemotherapy. Thorac. Cancer *12*, 1570–1578.
48. Deng, S., Zhang, H., Zhu, K., Li, X., Ye, Y., Li, R., Liu, X., Lin, D., Zuo, Z., and Zheng, J. (2021). M6A2Target: a comprehensive database for targets of m6A writers, erasers and readers. Briefings Bioinf. *22*, bbaa055.

STAR★METHODS

KEY RESOURCES TABLE

REAGENT or RESOURCE	SOURCE	IDENTIFIER
Antibodies		
Rabbit ploYclonal anti-B7-H3	Proteintech	Cat# 14453-1-AP; RRID: AB_2073577
Mouse monoclonal anti- GAPDH	Proteintech	Cat#60004-1-Ig; RRID: AB_2107436
Rabbit polyclonal anti-N-cadherin	Proteintech	Cat# 22018-1-AP; RRID:AB_2813891
Mouse monoclonal anti-YTHDF1	Proteintech	Cat#66745-1-Ig; RRID:AB_2882093
Mouse monoclonal anti-METTL3	Proteintech	Cat#67733-1-Ig; RRID: AB_2918502
Rabbit polyclonal anti-Ki67	Proteintech	Cat#27309-1-AP; RRID: AB_2756525
Rabbit monoclonal anti-MMP2	Abcam	Cat# ab92536; RRID: AB_10561597
Rabbit monoclonal anti-MMP9	Abcam	Cat# ab76003; RRID: AB_1310463
Mouse monoclonal anti-CD133	Abcam	Cat# ab27699; RRID: AB_940852
Mouse monoclonal anti-MYC	Abcam	Cat# ab18185; RRID: AB_444307
Rabbit polyclonal anti-Nanog	Novus	Cat#NB100-58842; RRID:AB_877697
Rabbit polyclonal anti-SOX2	Novus	Cat#NB110-79875; RRID: AB_1110593
Rabbit polyclonal anti-ALDH	Abcepta	Cat#AP1465C; RRID: AB_2223902
Mouse monoclonal anti-E-cadherin	OriGene	Cat#TA800692; RRID: AB_2625616
Mouse monoclonal anti-Slug	OriGene	Cat#TA800167; RRID: AB_2625278
Chemicals, peptides, and recombinant proteins		
BCA	Beyotime	Cat#P0012
Lipofilter™	Hanbio	Cat#HB-TRLF-5000
PMSF	Solarbio	Cat#P0100
CCK8 kit	Dojindo	Cat#CK04-11
EdU reagent	RiboBio	Cat#C10310
Murine RNase Inhibitor	Yeasen	Cat#10603ES05
RIPA	Crystal Color Biological	Cat#JC-PL001
TRIeasy reagent	Yeasen	Cat#10606ES60
Deposited data		
phs000178	TCGA – COAD	https://portal.gdc.cancer.gov/projects/TCGA-COAD
phs000178	TCGA – READ	https://portal.gdc.cancer.gov/projects/TCGA-READ
RM2Target_1141740	RIP-Seq	http://rm2target.canceromics.org/#/detail/RM2Target_1141740
RM2Target_1141741	CLIP-Seq	http://rm2target.canceromics.org/#/detail/RM2Target_1141741
Experimental models: Cell lines		
Colorectal cancer cell line HCT116	Wuhan Procell Life Science and Technology Co., Ltd	CL-0096
DLD1	Wuhan Procell Life Science and Technology Co., Ltd	CL-0074
SW620	Shanghai Fuheng Biotechnology Co., Ltd	FH0021

(*Continued on next page*)

Continued

REAGENT or RESOURCE	SOURCE	IDENTIFIER
SW480	Shanghai Fuheng Biotechnology Co., Ltd	FH0022
LOVO	Shanghai Fuheng Biotechnology Co., Ltd	FH0023
CACO2	Shanghai Fuheng Biotechnology Co., Ltd	FH0029
Experimental models: Organisms		
Nude mice	Jiangsu Jicui Pharmaceutical Health Biotechnology Co., Ltd	N/A
Software and algorithms		
SPSS software	SPSS Inc.	Version 26.0
Prism	GraphPad Software	Version 8.0.0
R software	Comprehensive R Archive Network	Version 4.0.4
Biological samples		
Colorectal cancer tissue and normal paracancerous tissue	The First Hospital of Lanzhou University	N/A

RESOURCE AVAILABILITY

Lead contact

The relevant experimental reagents, experimental methods and related data of this study should be directed to and will be fulfilled by the lead contact, Quan-lin Guan (guanql@lzu.edu.cn).

Materials availability

The study did not generate new unique reagents.

Data and code availability

- The Gene expression data for colon adenocarcinoma (COAD) and rectal adenocarcinoma (READ) were obtained from the TCGA database (https://portal.gdc.cancer.gov/). RIP-Seq and CLIP-Seq data have been deposited at the m6A2Target database (http://m6a2target.canceromics.org/) and are publicly available as of the date of publication. Accession numbers are listed in the key resources table.
- This paper does not report original code.
- Any additional information required to reanalyze the data reported in this paper is available from the lead contact upon request.

EXPERIMENTAL MODEL AND STUDY PARTICIPANT DETAILS

Clinical samples

Primary tumor and para cancerous tissues of patients with CRC were collected from the Department of Colorectal Surgery, First Hospital of Lanzhou University. Patients (aged 18-75 years) with CRC have no restriction on gender, ancestry, race or ethnicity or socioeconomic information. None of the enrolled subjects had received radiotherapy or chemotherapy, and no other cancer co-morbidities. **Cohort 1:** Ten pairs of fresh CRC and adjacent tissues were cryopreserved and used for quantitative analysis of B7-H3 mRNA using reverse transcription quantitative PCR (RT-qPCR). **Cohort 2:** A total of 109 pairs of formalin-fixed and paraffin-embedded CRC and adjacent tissues were used to detect B7-H3 protein expression using IHC. **Cohort 3:** B7-H3 protein expression in 14 pairs of fresh CRC tissues and matched adjacent tissues was evaluated using western blotting. The study was performed in strict compliance with the Declaration of Helsinki and approved by the Ethics Committee of the First Hospital of Lanzhou University (No. LDYYLL2020-113). All the patients provided written informed consent.

Animals

The male BALB/c nude mice, aged 4 weeks, were procured from Jiangsu Jicui Pharmaceutical Health Biotechnology Co., Ltd and cultured in a warm and moist-specific pathogen-free room with a 12 h light/dark cycle as well as ample food and water. This study was approved by the Animal Ethics Committee of the First Hospital of Lanzhou University (No. LDYYLL2020-113). All experimental procedures adhered to the "Care and Use of Laboratory Animals" guidelines.

METHOD DETAILS

Cell culture

Human CRC cell lines (DLD1, HCT116, SW620, LOVO, SW480, and CACO2) and normal human colon epithelial cell lines (FHC) were cultured in RPMI 1640 medium (GIBCO, USA) and the 293T cell line was cultured in basic DMEM medium (GIBCO, USA). All media were supplemented with 10% fetal bovine serum (FBS) (GIBCO, USA), 100 U/mL penicillin, (Beyotime, Shanghai, China) and 200μg/mL streptomycin (Beyotime, Shanghai, China). All cells were maintained at 37°C in a humidified atmosphere containing 5% CO_2.

RT-qPCR

Total RNA was extracted from the cells and tissue samples using TRIeasy™ Total RNA Extraction Reagent (Yeasen, Shanghai, China) according to the manufacturer's instructions. RNA was reverse-transcribed into cDNA using the Hifair® III 1st Strand cDNA Synthesis SuperMix for qPCR (Yeasen, Shanghai, China). The acquired cDNAs were then used as templates for RT-qPCR analysis using Hieff® qPCR SYBR® Green Master Mix (Yeasen, Shanghai, China). Quantification of the relative expression for mRNAs was calculated using the $2^{-\Delta\Delta Ct}$ method with the levels normalized to GAPDH mRNA.[43] All experiments were performed in triplicate. The primers used in this study are listed in Table S2.

Western blotting

Radio immunoprecipitation assay (RIPA, Crystal Color Biological, Xi'an, China) lysis buffer supplemented with protease inhibitors (PMSF, Solarbio, Beijing, China) was used to extract total protein from CRC cells and tissues. Total protein was fractionated using 10% SDS-PAGE and transferred onto 0.45 μm polyvinylidene difluoride (PVDF) membranes (Millipore, Boston, MA, USA). After blocking by 5% non-fat milk in TBST for 1 h, the membranes were incubated at 4 °C overnight using the corresponding diluted primary antibodies. The following day, the membranes were imaged after incubation with appropriately diluted secondary antibodies at room temperature for 1 h. The immunoblots were detected using an Odyssey® Infrared Imaging System (LI-COR Biotechnology, Lincoln, NE, USA). The antibodies used are summarized in Table S3.

Lentiviruses and cell transfection

Short hairpin RNAs (shRNAs) targeting B7-H3, METTL3, YTHDF1 (sh-B7-H3, sh-METTL3, or sh-YTHDF1), and a negative control (sh-Ctrl) were chemically synthesized by GenePharma (Shanghai, China). The shRNA constructs were generated by inserting shRNA fragments (B7-H3, METTL3 and YTHDF1) into shLenti vectors (HBLV-h-B7H3-3×FLAG-Luc-Puro or pSIH1-H1-copGFP-T2A-Puro) (Hanbio Biotechnology, China). Overexpression constructs were generated by inserting fragments of the full-length coding region (B7-H3, YTHDF1) into HBLV-h-B7H3-3×FLAG-Luc-Puro or pCDH-CMV-MCS-EF1-CopGFP-T2A-Puro plasmids (Hanbio Biotechnology, China). The constructs were transfected into 293T cells (Fuheng Institute of Biotechnology, Shanghai, China) using the Lipofiter™ Kit (Hanbio Biotechnology, China). Next, shRNA or overexpression lentiviruses were used to infect the CRC cells. After 3 days of transfection, 5μg/mL puromycin was added to screen successfully transfected cells. The knockdown and overexpression efficiencies were quantified using RT-qPCR and western blotting assays. The shRNA sequences are listed in the Table S4.

Cell growth and proliferation assays

Cell viability was assessed by cell counting kit-8 (CCK-8), 5-ethynyl-2′-deoxyuridine (EdU) labeling and colony formation assays. For the CCK-8 assay (DOJINDO, Tokyo, Japan), 1×10^3 cells were seeded into 96-well plates. After incubation for 24h, 48h, 72h, 96h or 120h, respectively, 10μL of CCK-8 was added to the wells and incubated for another 4 h at 37°C. Cell viability was evaluated by measuring the optical density (OD) value at 450nm using a microplate reader (BioTek Instruments, Winooski, VT, USA). All experiments were performed out in triplicate.

EdU labeling assays were conducted according to the instructions of the EdU Cell Proliferation Assay Kit (RiboBio, Guangzhou, China). Cells were first incubated with 35–50μM EdU solution at room temperature for 2h. Subsequently, the cells were fixed with 4% neutral paraformaldehyde for 30 min at room temperature and then 0.25–0.35 mL of 2 mg/mL glycine solution was added to each well. The cells were then decolorized for 5min, permeabilized with PBS containing 0.5% Triton X-100 for 20 min and washed thrice with PBS. Finally, the cells were stained with Apollo staining reagent for 30 min. Nuclei were stained with 4′, 6-diamidino-2-phenylindole (DAPI, Solarbio, Beijing, China). Images were captured using a fluorescence microscope (Nikon, Tokyo, Japan).

For the colony formation assay, cells were seeded in 6-well plates at a density of 1×10^3 cells/well. After two weeks, the colonies were collected, fixed with 4% paraformaldehyde, and stained with 1% crystal violet (Sigma-Aldrich, USA). Colony-forming units were recorded and photographed under a microscope (Nikon Eclipse, Japan).

Transwell assay

Cells invasion was analyzed using a 24-well Transwell chamber system (Corning, USA). Cells (5×10^4/well) were seeded with 0.2 mL serum-free culture medium in the apical chambers pre-coated with Matrigel (Corning, USA), and 0.6mL culture medium containing 15% FBS was added to the basolateral chambers. After incubation for 30h, the cells were fixed in cold methanol for 5min and stained with 0.1% crystal violet (Sigma-Aldrich, USA) for 30min. After rinsing with water, chamber membranes were mounted and covered with slides. The invading cells were imaged and counted under a microscope at 100×magnification using six random of view.

Wound healing assay

A wound healing assay was performed to analyze cell migration. The treated cells were seeded into the 6-well plates (Corning, USA) until they reached 90% confluence. The cells were then scratched using a pipette tip and cultured in FBS-free medium for 36h. The detached cells were washed with PBS, and wound widths at 0h and 36h were examined under a light microscope (Nikon Eclipse, Japan). Image-Pro Plus software (Image Pro Plus Software Inc., MD, USA) was used to measure the relative distance of wound closure.

Methylated RNA immunoprecipitation-qPCR (MeRIP-qPCR)

Total RNA was extracted from CRC cells with METTL3 knockdown or empty vector control (sh-METTL3/sh-Ctrl) and treated with DNase (Yeasen, Shanghai, China) to remove genomic DNA. After mRNA purification and fragmentation, the fragmented RNA (100 nucleotides) was incubated with an m6A primary antibody (ab208577, Abcam, UK) for immunoprecipitation using a MeRIP m6A Kit (Merck Millipore, Germany). The mRNA with m6A enrichment was then assayed using RT-qPCR. The primers used for MeRIP-qPCR are listed in Table S2.

Animal experiments

All animal experiments were approved by the Animal Ethics Committee of the First Hospital of Lanzhou University. All experimental procedures adhered to the "Care and Use of Laboratory Animals" guidelines. The male BALB/c nude mice, aged 4 weeks, were procured from Jiangsu Jicui Pharmaceutical Health Biotechnology Co., Ltd. Approximately 1×10^7 CACO2 cells stably expressing sh-B7-H3 or scrambled shRNA were subcutaneously injected into the mice (5 per group). Tumor width and length were measured every three days, and tumor volume was calculated as (length×width^2)/2. After 29 days, the mice were euthanized, and the xenograft tumors were surgically dissected for H&E staining and IHC assays and weighed. Tumor weights were measured on the 29th day after subcutaneous transplantation.

The mRNA stability assay

CRC cells were incubated in 6-well plates for 24h until 50% confluence, followed by treatment with 5 μg/mL actinomycin D (Sigma-Aldrich, USA) for 0h, 3h, or 6h, respectively. Total RNA was isolated and analyzed using RT-qPCR. The mRNA degradation rate was calculated based on the previously mentioned protocols.[44]

Tumor sphere formation assay

For the oncosphere formation assay, 1×10^3 cells were seeded in each well of the ultra-low attachment 6-well plates (Corning, NY, USA) in DMEM/F-12 supplemented with B-27 serum replacement (1:50, Invitrogen, USA), 20ng/mL human recombinant EGF (Sigma-Aldrich, USA), and 20ng/mL bFGF (Sigma-Aldrich, USA). After 7days of cell culture, spheres larger than 50μm in diameter were counted at 40×magnification under an inverted microscope (Nikon Eclipse, Japan).

H&E and IHC staining

H&E staining was performed on 5-μm paraffin-embedded tissue sections following a standard H&E staining protocol.[45] Tissue samples were fixed, embedded, cut into sections, dewaxed, antigen retrieved, incubated with primary antibodies, incubated with secondary antibodies, DAB-stained, counterstainied with hematoxylin, dehydrated, made transparent and mounted with neutral gum. The primary antibodies used were anti-B7-H3 (1:400; Proteintech, Cat No. 14453-1-AP), anti-ALDH (1:100; Abcepta, Cat No. AP1465c), anti-CD133 (1:500; Abcam, Cat No. ab27699), anti-MYC (1:500; Abcam, Cat No. ab18185), anti-NANOG (1:500; Novus, Cat No. NB100-58842), anti-SOX2 (1:300; Novus, Cat No. NB110-79875), anti-Ki67 (1:200; Proteintech, Cat No. 27309-1-AP), anti-Slug (1:1000; OriGene, Cat No. TA800167), anti-N-cadherin (1:5000; Proteintech, Cat No. 22018-1-AP) and anti-E-cadherin (1:2000; OriGene, Cat No. TA800692). Two experienced pathologists independently reviewed and scored all the sections. The IHC score was calculated using a modified Histoscore (H-score).[46] This method was used to evaluate the semi-quantitative expression of target proteins using the following formula: immunoreactivity score = staining intensity score (0: no staining, 1: weak, 2: moderate, and 3: strong staining) × proportion of positive cells score.[47] The expression level of target proteins was considered "low expression" if the H-score was 0–4 and "high expression" if the score was 5–9.

Bioinformatics analyses

Gene expression data for colon adenocarcinoma (COAD) and rectal adenocarcinoma (READ) were obtained from the TCGA database (https://portal.gdc.cancer.gov/). The m6A2Target database, which is a database of m6A-modified target gene sets that have been validated through the Bindind or Perturbation module, including (writer/eraser/reader) targets. Through the binding module, based on the crosslinking-immunoprecipitation and high-throughput sequencing (CLIP-Seq) technology conducted in Hela and A549 cells (http://m6a2target.canceromics.org/)[48] was used to screen m6A-related mRNAs. SRAMP (http://www.cuilab.cn/sramp), a site prediction tool based on a random forest machine learning framework, was used to predict the post-transcriptional m6A modification sites. The m6A locus was predicted using a target sequence. Pearson's analysis for determining the correlation of B7-H3 and YTHDF1 was calculated using the "ggstatsplot" and "ggplot2" packages. The 'forestplot' package, available in R, was used to identify each variable's *P* value, hazard ratio (HR), and 95% confidence interval (CI).

QUANTIFICATION AND STATISTICAL ANALYSIS

Data are presented as mean ± standard deviation (SD). Student's *t*-test was used to compare the differences between every two groups. One-way ANOVA was used for multiple group comparisons. The χ^2 test or Fisher's exact test was applied for categorical variables. Kaplan–Meier curves and log-rank tests were used for survival analysis for CRC patients. All data were analyzed using R (version 4.0.4; www.r-project.org), SPSS 26.0 (SPSS Inc., Chicago, IL, USA) and GraphPad Prism 8.0 (Graph-Pad Software, USA). Statistical significance was set at as **P*<0.05, ***P*<0.01, ****P*<0.001, and *****P*<0.0001. All experiments were performed in triplicate.